Water Resources and Industry ∎ (∎∎∎∎) ∎∎∎–∎∎∎

Contents lists available at ScienceDirect

Water Resources and Industry

journal homepage: www.elsevier.com/locate/wri

Titania coated silica nanocomposite prepared via encapsulation method for the degradation of Safranin-O dye from aqueous solution: Optimization using statistical design

Basanti Ekka, Manoj Kumar Sahu, Raj Kishore Patel*, Priyabrat Dash*

Department of Chemistry, National Institute of Technology, Rourkela, Odisha -769008, India

ARTICLE INFO

Article history:
Received 29 March 2016
Received in revised form
6 August 2016
Accepted 18 August 2016

Keywords:
TiO_2 coated silica nanoparticles
Photodegradation
Safranin O
Response surface methodology
Central composite design

ABSTRACT

Titania coated silica nanoparticles, which were synthesized via nanoparticle encapsulation route, are employed to degrade safranin-O dye from aqueous solution under UV light irradiation and were characterized by FT-IR, XRD, FESEM, N_2 adsorption-desorption method and Zeta potential measurement. The results showed that the nanoparticles have a core-shell structure composed of about 100 nm of diameter of silica with several TiO_2 fine particles in shell. After the degradation, this process is optimized through the response surface methodology (RSM). In this response study, photodegradation efficiency was evaluated by three main independent parameters such as catalyst dose, initial dye concentration and reaction time. Parameter sensitivity studies of the degradation efficiency of titania coated silica nanoparticles have shown 93.29% degraded under the optimal conditions of catalyst dose of 89.80 mg/g, initial dye concentration of 17.61 mg/L and reaction time of 12 min. We cross-checked the predicted values of degradation efficiency with the experimental values and were found to be in good agreement (R^2=0.9983 and adj-R^2=0.9967).

1. Introduction

Over the past decades, water pollution caused by organic dyes produced from textile and other industrial processes have been attracted much attention due to a considerable damage to human beings and aquatic animals. These organic dyes result in high chemical oxygen demand (COD), bad smell, and mainly are responsible for the colouration of wastewaters [1,2]. Among many dyes that are applied in manufactured products, safranin-O (SO) must be highlighted. Safranin-O is a basic dye and is widely used for food coloring additive, a dye for silk, jute, leather, wool, cotton, paper, and also in manufacturing of paints and printing inks [3–5]. Various physical, chemical and biological techniques have applied for treatment of dye-containing wastewater such as: incineration, biological treatment, ozonation, adsorption on solid phases etc.[6–11].

Though the above mentioned methods work well in some instances, these methods have some limitations like production of toxic volatiles, non-degradable sludge and bad smell [12–14]. To eliminate these disadvantageous and adverse effects created by in-situ products, the heterogeneous photocatalysis became, an elegant alternative for degradation of organic dyes [15,16]. In contrast to the traditional methods, photocatalytic technique in wastewater treatment is superior

* Corresponding authors.
E-mail addresses: rkpatel@nitrkl.ac.in (R.K. Patel), dashp@nitrkl.ac.in (P. Dash).

http://dx.doi.org/10.1016/j.wri.2016.08.001

due to quick oxidation, no formation of polycyclic products and oxidation of pollutants in the ppb range [17,18]. By the way, the photocatalysis may be defined as a process in which a semiconductor material absorbs energy of light more than or equal to its band-gap, thereby generating electrons and holes that can further generate free-radicals in the system to oxidize the substrate [19]. Many photocatalysts have been synthesized and employed to degrade organic pollutants such as ZnO, Nb_2O_5, SnO_2, Ni_2O_3, Bi_2O_3, Al_2O_3, TiO_2 etc. [20–26]. Among these catalysts, TiO_2 is widely used as a photocatalyst due to its high potential in reducing environmental contaminant by decomposing organic and inorganic pollutants because of its wide band gap, chemical stability, nontoxicity and low cost [27–29]. However, there are several drawbacks associated with the photocatalytic efficiency of TiO_2. A key challenge of photocatalysis in the application of these nanoparticles is the agglomeration which can cause the deactivation of the catalysts and separation. Furthermore, owing to thermally unstable, they can undergo phase transformation and crystallite growth at high temperature. These process leads to a reduction in the surface area [30]. Several attempts have been made to overcome these problems by doping with different metals and non-metals such as Ag, Pd, Sn, C, N, etc. [31–35]. Though the doping increased active surface area dramatically, the problem of separation of catalyst is still a major concern.

Recently, researchers focused on the synthesis of concentric multilayer semiconductor nanoparticles known as core/shell nanoparticles [36]. Core/shell nanoparticles have gained great interest due to their improved chemical and physical properties as compared to the counterpart studies. Moreover, the titania morphologies can be tailored by loading titania on inert supports like zeolites, glass fibers and beads, carbon fibers, alumina and silica in the advanced photocatalytic degradation of pollutants. Among these supporting materials, mesoporous silica have recently attracted much attention for promising application such as catalysis, separations, drug delivery, and microelectronics due to its high surface area [37,38]. Furthermore, besides being silica has no absorption in UV range, it is easy to synthesize mesoporous silica with a high specific surface area and pore volume. The advantages of titania coated silica materials are high specific surface areas, large pore volumes and narrow pore size distribution and high thermal stability. Due to these properties, the titania coated silica materials exhibit higher absorption capacity and better photocatalytic oxidation of various organic pollutants.

In spite of these advantages, it is still a challenge to search for new and better techniques for large-scale synthesis of SiO_2-TiO_2 core-shell photocatalysts with high surface area, controlled pore size and morphology. Traditional synthetic methods involves the deposition of metal precursors onto high surface area supports for synthesis of supported nanoparticle catalysts, followed by various thermal activation treatments. The uniform distribution of nanoparticles and the degree of dispersion of nanoparticles on the support are each highly dependent on the pH and concentration of the precursor solution, type of the oxide support, and calcination temperature. In addition, these methods often provide limited control over the composition and structures of supported nanoparticle catalyst, which often leads to significant compositional non uniformity from particle to particles. In order to address these issues, we fabricated titania coated silica nanoparticles following the nanoparticle encapsulation method. In this method titania was incorporated into pre-synthesized silica nanoparticles by sol-gel method. This route provides an unconventional method of designing supported nanoparticle catalysts through a rational chemical approach, which gives well dispersion of TiO_2 nanoparticles within high surface area silica supports and good control over the size, composition and internal structure of the nanoparticles. Among the various techniques available for the synthesis of core/shell nanoparticle catalysts, the process of entrapping the pre-synthesized nanoparticles into an inorganic matrix by the sol-gel method is an interesting route [39]. This method takes advantage of the large number of synthetic solution protocols that have been developed to carefully control nanoparticle size, shape, and composition. So far, the synthesis of titania coated silica nanoparticles using the encapsulation method has not been studied in detail.

The efficiency of photocatalytic degradation depends on several parameters such as the catalyst dose, initial dye concentration, the reaction time, pH of the solution, the molecular structure of the dye used, etc. In the conventional methods, experiments were carried out by one-at-a-time sensitivity experiments which leads to unpredictable number of experiments. To overcome this problem with considerable accuracy, models such as Design Expert (DE) are employed for obtaining the optimized conditions with the less time and reducing chemical cost. Among various experimental design methodologies, Response Surface Method (RSM) is efficient and can measure the relationship among the controllable input parameters and to obtain response surfaces [40]. RSM has the potential to estimate linear, interaction and quadratic effects of the factors and it can predict model for the response. It can also analyse the process and gives the results faster than the conventional one-factor-at-a-time approach [41]. The experimental data required are reliant on the chosen design: central composite or Box–Behnken designs [42]. The design technique for RSM is as follows: (i) Performing a bunch of runs of experiments for adequate and dependable measurement of the response of interest. (ii) Emerging a mathematical model of the second-order response surface with the best fit. (iii) Determining the best set of experimental parameters, which can produce a maximum value of response. (iv) Representing the interactive effects of process parameters through two and three-dimensional plots [43].

The present work reports the novel technique for synthesis of titania coated silica nanocomposite with high surface area and high thermal stability (900 °C) i.e. nanoparticle encapsulation method which provides better control over nanoparticles size and structure. The synthesized novel photocatalyst was used for photodegradation of safranin-O dye, which is phenazine dye, widely used in textile industry. This is for the first time, the experimental data has been validated by theoretical modeling with response surface methodology (RSM) to optimize the degradation process of safranin-O dye, using titania coated silica nanocomposite, which has not been studied yet. The variable factors investigated were the catalyst dose, initial dye concentration and reaction time. The photocatalytic degradation efficiency was checked by a UV–vis spectrophotometer.

Please cite this article as: B. Ekka, et al., Titania coated silica nanocomposite prepared via encapsulation method for the degradation of Safranin-O dye from aqueous solution: Optimization using statistical design, Water Resources and Industry (2016), http://dx.doi.org/10.1016/j.wri.2016.08.001

The results of our optimization demonstrate that the RSM can be used readily to determine the optimal conditions for the degradation of safranin-O dye.

2. Experimental

2.1. Materials

Cetyltrimethylammonium bromide (CTAB), tetraethyl orthosilicate (TEOS) and titanium tetraisopropoxide (Ti(OCH $(CH_3)_2)_4$) were obtained from Sigma-Aldrich whereas Degussa P25, methanol, ethanol, sodium hydroxide, ammonium hydroxide, ammonium nitrate and safranin-O (SO) were obtained from HIMEDIA. All chemicals employed for this experiments are of analytical grade and were used without any further purification.

2.2. Synthesis of silica nanoparticles

In this synthesis, 0.29 g of CTAB was dissolved in 0.512 M 150 mL of ammonium hydroxide solution at 40 °C. Then, 2.5 mL of 0.88 M ethanolic TEOS was added to the solution under vigorous stirring. After 1 h, the solution was aged at 40 °C for 18 h in static conditions, so it has become colloid. The synthesized colloid then washed off the CTAB with 50 mL of ethanolic ammonium nitrate solution twice to make sure the complete removal.

2.3. Synthesis of titania coated silica nanoparticles

0.25 mL (5 vol%) of water was added to the prepared silica nanoparticles in a beaker and stirred. 2.02 mL of Ti(OCH $(CH_3)_2)_4$ is taken as the titanium precursor and was added to 5 mL of freshly dried methanol using hot molecular sieves. This was then added to the beaker and gel was formed within 10–15 min. This was then kept for aging overnight and followed by drying at the temperature between 150 and 200 °C for 1–2 h. The dried gel was then powdered using mortar and pestle and calcined in air at a temperature of 900 °C for 3 h.

2.4. Characterizations

The FT-IR spectroscopy (Perkin-Elmer) was used to determine the bonding between titania and silica in nanocomposites. The crystal structure of the synthesized catalyst was determined by X-Ray diffractometer (XRD) of RIGAKU JAPAN/ULTIMA-IV with CuK_α source. The size, morphology and structure of the nanoparticle were investigated by field emission scanning electron microscopy (FESEM), subsequently the chemical composition of the prepared nanoparticle was measured by EDX performed in Nova NANOSEM/FEI. The surface area was calculated by using the BET (Brunauer–Emmet–Teller) equation in quantachrome autosorb (IQ) model ASIQM0000-4. The pore size distribution and pore volume were obtained by applying the BJH (Barrett–Joyner–Halenda) method. The samples were degassed in vacuum at 150 °C. All the samples were dispersed into deionized water and the zeta potential measurements were taken by zeta sizer nano (MALVERN ZS 90).

2.5. Photocatalytic study of safranin-O dye using titania coated silica nanoparticles

The photocatalytic studies were conducted in a reaction chamber (50 cm x 50 cm x 50 cm) containing an artificial UV light (15 W bulb of Philips). The distance between the lamp and the surface of the solution was about 15 cm. The photocatalytic degradation of SO dye was measured by adding a known amount of catalyst to the dye solution prepared in DI water. The mixture was stirred in the dark for 30 min to obtain an equilibrium photocatalyst-dye solution. From this mixture, a small quantity was then taken out at regular intervals with a syringe and was centrifuged at 8000 rpm for 10 min to remove the catalyst. The supernatant was taken and filled in a quartz cuvette without dilution and was then studied using UV–vis spectroscopy to calculate the concentration of SO dye.

3. Results and discussion

3.1. Structure and morphology characterization

In this work, silica nanoparticle was prepared as discussed in the experimental section. Later on, the nanoparticle encapsulation method was employed for the fabrication of titania coated silica nanoparticle. The photocatalytic activity of the synthesized material was examined by employing safranin-O dye as a model pollutant. Safranin-O dye belongs to quinone-imine class, which is widely used in textile industry. Safranin-O dye discharged from textile industry poses a big threat to our environment, since the dye is known for its carcinogenic nature even in trace amounts. The presence of various chemical and physical properties of the catalyst was then characterized by different characterization techniques.

FT-IR spectra, of titania coated silica nanoparticles are shown in Fig. 1. The presence of water is evidenced by the

Please cite this article as: B. Ekka, et al., Titania coated silica nanocomposite prepared via encapsulation method for the degradation of Safranin-O dye from aqueous solution: Optimization using statistical design, Water Resources and Industry (2016), http://dx.doi.org/10.1016/j.wri.2016.08.001

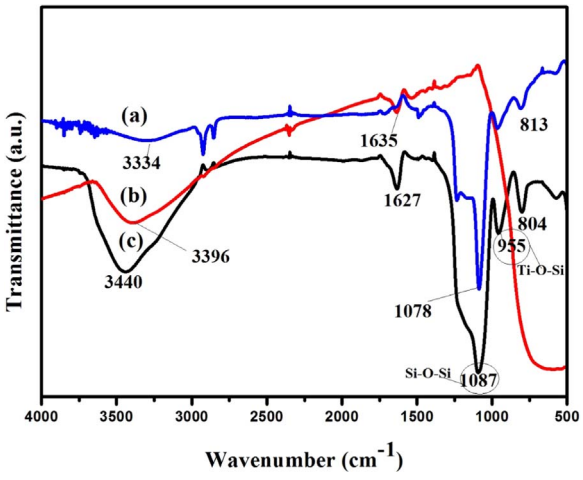

Fig. 1. FTIR spectra of (a) silica nanoparticles (b) titania nanoparticles (c) titania coated silica nanoparticles.

appearance of the OH stretching at 3440 cm^{-1}. The peak at 1627 cm^{-1} indicates the bending vibration of Si–OH bond. The presence of hydroxyl ions on the surface of the catalyst is advantageous for the photocatalytic activity of TiO_2 because it offers higher capacity for oxygen adsorption [44]. In Fig. 1(c), new distinct and sharp peaks around 1087 cm^{-1} and 804 cm^{-1} ascribed to asymmetric stretching and symmetric bending of Si–O–Si vibration respectively. An absorption peak at 955 cm^{-1} is attributed to the Si–O–Ti group in titania coated silica nanoparticle indicating the formation of Si–O–Ti bond [45]. The formation of Si–O–Ti bond arises from two possibilities, first may be due to the substitution of small amount of Ti (IV) for Si (IV) in the frame work of mesoporous silica and second, may be due to the connection of embedded titania particles to the mesoporous silica matrix through the Si–O–Ti bonds in the interface between silica and titania [46]. The alkyl groups have been removed by calcination and it is evident by the absence of the C-H peaks in the FTIR spectra of titania coated silica nanoparticles.

The X-ray diffraction patterns (XRD) of titania coated silica nanoparticles is found to possess a fine nano-crystalline titania anatase phase, which is shown in Fig. 2. The diffraction pattern having a peak at 2Θ values of 25.3°, 37.8°, 48.0°, 53.9°, 55.1°, 62.7°, 70.2°, 75.2° correspond respectively to [101], [004], [200], [105], [211], [204], [220], [215] crystal planes which can be indexed to the anatase phase of TiO_2 which matches well to the reported JCPDS data (Card No. 71-1166). During hydrothermal treatment, TiO_2 changes its phase to anatase by dissolution and reprecipitation processes, in which transiently dissolved titanate species rapidly nucleated to form nanocrystalline structure because of the high reactivity of the hydrothermal system. Presence of silica improved the thermal stability of titania, as a result very few rutile phase has occurred at high calcination temperature (900 °C). It is observed that the electron transport is faster in the anatase phase of TiO_2 than the rutile phase of TiO_2, leading to an enhanced photocatalytic performance [47]. The small hump located at 22° can be assigned to the characteristic peak of amorphous silica (JCPDS Card No. 49-1711). In addition, the presence of SiO_2 stabilized the anatase phase of TiO_2 even at 900 °C [48,49]. The average crystallite size of TiO_2 nanoparticles were calculated for [101] crystal plane using the Scherer equation (R m=k λ/β1/2 cosθ) and is found to be 6 nm.

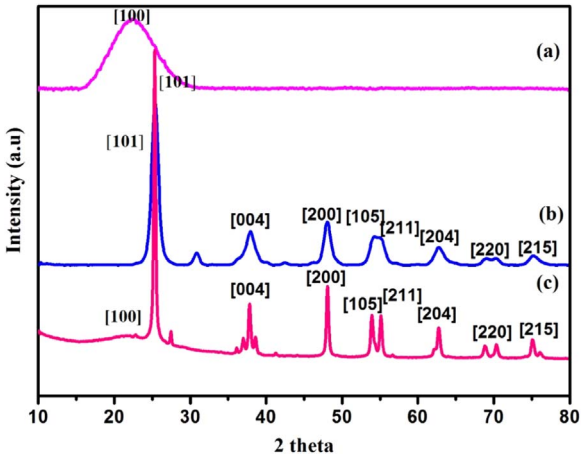

Fig. 2. X-ray powder diffraction patterns of (a) silica nanoparticle (b) titania nanoparticle (c) titania coated silica nanoparticles.

Please cite this article as: B. Ekka, et al., Titania coated silica nanocomposite prepared via encapsulation method for the degradation of Safranin-O dye from aqueous solution: Optimization using statistical design, Water Resources and Industry (2016), http://dx.doi.org/10.1016/j.wri.2016.08.001

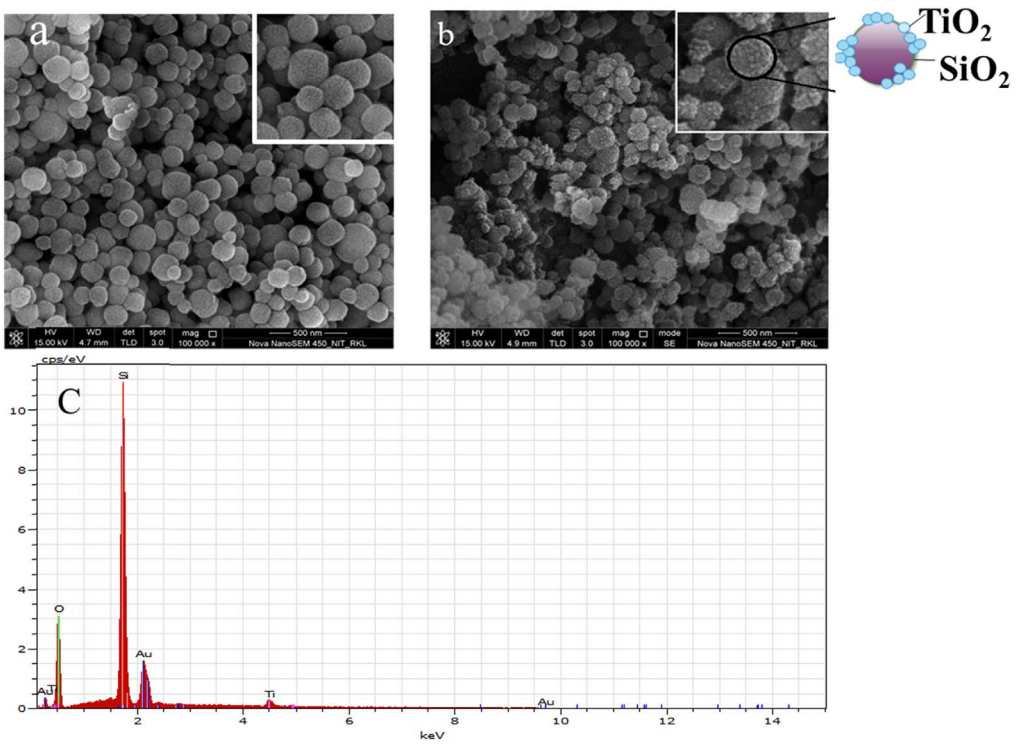

Fig. 3. FESEM images of (a) silica nanoparticle (b) titania coated silica nanoparticle, and (c) EDX spectrum of titania coated silica nanoparticle.

The detailed size and morphology of the titania coated silica nanoparticle further investigated by the field emission scanning electron microscopy (FESEM) and corresponding EDX spectrum, which is shown in Fig. 3(a–c). The FESEM image (Fig. 3(a)) shows that the pure silica nanoparticles were intact spheres with the smooth surface without aggregation. Further it was found from FESEM images that the silica particles preserved their particulate form after calcination at 900 °C and the SiO_2 core was successfully coated with a thin layer of TiO_2 with several nanometers, resulting in a rough surface morphology (Inset Fig. 3(b)). A quantitative EDX spectrum was taken to determine the elemental composition of titania coated silica nanoparticle which is shown in Fig. 3(c). From the figure, it confirmed that there are no other elemental impurities present in the catalyst. Furthermore, the Si and Ti elements were calculated according to the data of atomic percent and found to be 39.5% and 2.0% respectively.

Fig. 4 shows the typical N_2 adsorption-desorption isotherm of SiO_2-TiO_2 nanoparticles. The isotherm represents the type IV isotherm according to the International Union of Pure and Applied Chemistry (IUPAC) nomenclature indicating the presence of mesopores in the composite which is related to capillary condensation associated with the pore channels. By

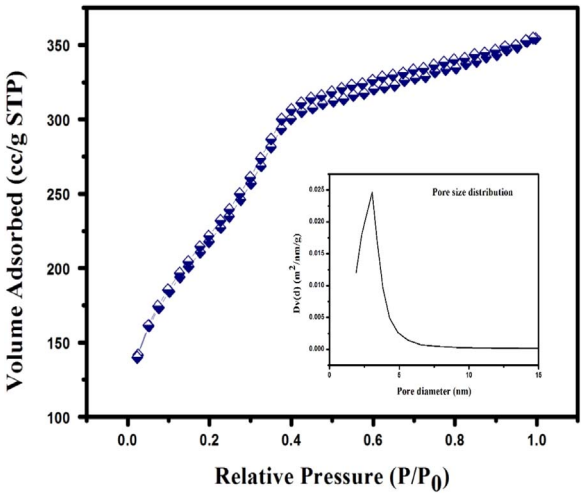

Fig. 4. N_2 adsorption-desorption isotherm and pore size distribution curve of titania coated silica nanoparticle.

Please cite this article as: B. Ekka, et al., Titania coated silica nanocomposite prepared via encapsulation method for the degradation of Safranin-O dye from aqueous solution: Optimization using statistical design, Water Resources and Industry (2016), http://dx.doi.org/10.1016/j.wri.2016.08.001

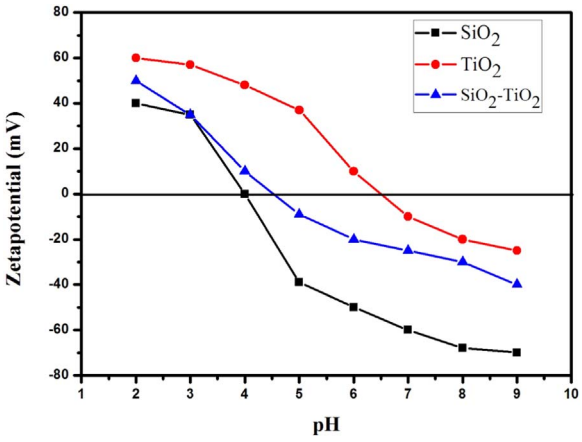

Fig. 5. Variation of zeta potential with pH values of pure silica, pure titania and titania coated silica nanoparticle.

analysing the N_2 adsorption-desorption isotherm, it was found that the catalyst has a high surface area of about 725 $m^2\ g^{-1}$ and pore volume of 0.142 cc g^{-1}. The BJH pore size distributions of the titania coated silica nanoparticles is shown in the inset of Fig. 4. The sample has a narrow pore size distribution and the average pore size is 3 nm, implying that the catalyst was mesoporous in nature.

In order to have a proper coating of titania on silica, the dispersion stabilities of the silica and titania are of high significance to prevent homo-coagulation. To achieve hetero-coagulation, surface charges are needed to be monitored via zeta potential measurements, and the results are shown in Fig. 5. Also, it can be seen that the zeta potential decrease as the pH of the solution increases and the order of decreases zeta potential is as: pure silica nanoparticles, titania nanoparticles and titania coated silica nanoparticles.

When the pH is higher than the isoelectric point (IEP), (due to the deprotonation) the surface and, therefore, the zeta potential of all above materials become negative. It was observed that the IEP of the titania coated silica nanoparticles ranged between those of pure silica nanoparticle (IEP at pH 3.8) and pure titania nanoparticles (IEP at pH 6.2). This confirmed that the titania particles got adsorbed on the silica surface and formed a non-complete (non-continuous) shell which was previously confirmed by FESEM, where the surface morphology of titania coated silica nanoparticle is rough, due to titania particles. A similar type of observation was found in the literature [50].

Before employing an experimental design, it was necessary to study the extents of photocatalytic degradation of safranin-O dye. Fig. 6 shows the photocatalytic degradation of the safranin-O dye using P25 (Degussa), pure titania, and titania coated silica nanoparticles under three different conditions: catalyst dose 100 mg, initial dye concentration 10 mg/L and reaction time 20 min. After 20 min, the concentration of safranin-O dye on P25 and pure titania did not decrease much with prolonged UV irradiation whereas titania coated silica nanoparticle showed enhanced degradation efficiency. This indicates that the affinity for safranin-O dye after deposition of TiO_2 nanoparticle on silica leads to the higher surface area which could be responsible for the higher catalytic activity of the catalyst.

3.2. Experimental design

Response surface methodology is a collection of statistical and mathematical techniques which is useful for developing, improving and optimizing the processes. The use of statistical experimental design techniques in the photocatalytic process can result in the requirement of fewer resources such as time, reagents and experimental work. In the present study of central composite design, which is a widely used form of RSM, was used for optimization of photodegradation of safranin-O dyes and three main factors chosen were: catalyst dose (mg/g) (X_1), initial dye concentration (mg/L) (X_2) and reaction time (min) (X_3) as shown in Table 1.

3.3. CCD model and residuals analysis

The 3-factor CCD matrix and experimental results obtained from Design Expert 7.1 software for the photocatalytic degradation of safranin-O is given in Table 2. The second-order polynomial response expression in (Eq. (1)) was used to correlate the dependent and independent variables:

$$Y = b_0 + b_1X_1 + b_2X_2 + b_3X_3 + b_{12}X_1X_2 + b_{13}X_1X_3 + b_{23}X_2X_3 + b_{11}X_1^2 + b_{22}X_2^2 + b_{33}X_3^2 \quad (1)$$

where Y is the response, b_0 is the constant, b_1, b_2 and b_3 are the linear coefficients, b_{12}, b_{13} and b_{23} are the cross-product coefficients, b_{11}, b_{22} and b_{33} are the quadratic coefficients.

Based on these results, an empirical relationship between the response and independent variables (parameters) are

Please cite this article as: B. Ekka, et al., Titania coated silica nanocomposite prepared via encapsulation method for the degradation of Safranin-O dye from aqueous solution: Optimization using statistical design, Water Resources and Industry (2016), http://dx.doi.org/10.1016/j.wri.2016.08.001

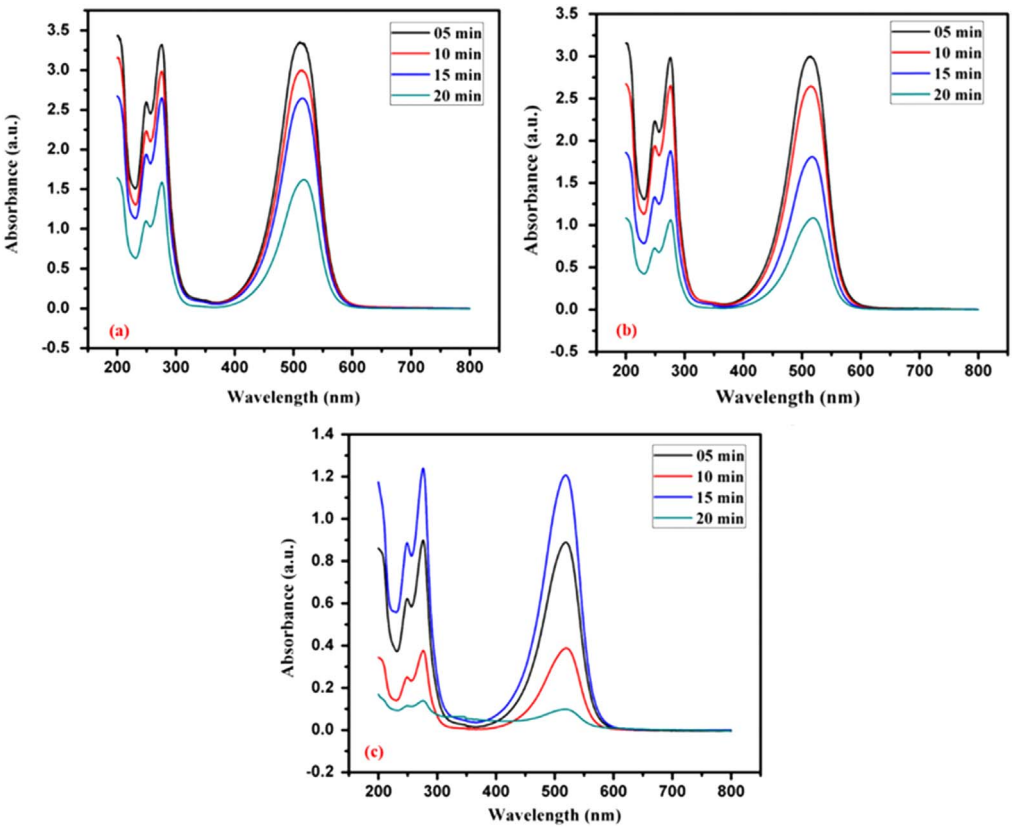

Fig. 6. Absorbance spectra of degradation of safranin-O dye with respect to time. (a) P25 (b) Pure TiO_2 nanoparticle (c) Titania coated silica nanoparticle.

Table 1
Values and levels of chosen variables for central composite design.

Variables	Ranges and levels				
	−2	**−1**	**0**	**+1**	**+2**
Catalyst Dose (mg)	32.95	50	75	100	117.04
Initial Dye Concentration (mg/L)	3.18	10	20	30	36.8
Reaction Time (min)	6.59	10	15	20	23.4

expressed by the second-order polynomial equation which consists of 10 statistically significant coefficients:

$$Y = 93.13 + 8.33X_1 - 3.97X_2 + 2.28X_3 + 0.54X_1X_2 + 0.54X_1X_3 + 0.29X_2X_3 - 9.65X_1^2 - 1.11X_2^2 - 1.50X_3^2 \quad (2)$$

Where Y is the response variable of degradation efficiency of safranin-O. The X_1, X_2 and X_3 represent three experimental factors viz. catalyst dose, initial dye concentration and reaction time respectively.

The photocatalytic degradation efficiency of safranin-O by titania coated silica nanoparticles with varied parameters within the selected range has been predicted by Eq. (1) and the analytical and predicted values are presented in Table 2. These results indicated good agreement between the experimental and predicted values of degradation efficiency of dyes. This can further be explained by plotting the experimental degradation efficiency versus predicted values, which is shown in Fig. 7. From Fig. 7, it is confirmed that all values are well distributed along the straight line, indicating that there is no non-normality. This validates that the established model is appropriate to explain the range of studied. Moreover, the predicted R^2 (correlation coefficient) is very close to the corresponding R^2 value of analytical experiments, which is shown in Table 3.

To evaluate the fitness, significance and adequacy of the model for this particular study, analysis of variance (ANOVA) has been applied to find the effects of each of the variable and interaction effect of parameters on the response (Table 3). The F value for the model was calculated to be 638.22, with lower probability (< 0.0001) indicating that the model is highly significant. There was only a 0.01% possibility that the model F value could happen due to noise. The model p value was < 0.0001, which further confirmed that the model is statistically significant, whereas the value greater than 0.1000 indicated

Please cite this article as: B. Ekka, et al., Titania coated silica nanocomposite prepared via encapsulation method for the degradation of Safranin-O dye from aqueous solution: Optimization using statistical design, Water Resources and Industry (2016), http://dx.doi.org/10.1016/j.wri.2016.08.001

Table 2
Experimental design matrix and the value of responses based on analytical and simulation experiments.

Standard order	Uncoded parameter			Coded parameter			Degradation efficiency (%)	
	A	**B**	**C**	**A**	**B**	**C**	Actual value	Predicted value
1	50	10	10	−1	−1	−1	75.75	75.61
2	100	10	10	1	−1	−1	90.39	90.10
3	50	30	10	−1	1	−1	66.22	66.00
4	100	30	10	1	1	−1	81.96	82.66
5	50	10	20	−1	−1	1	79.34	78.51
6	100	10	20	1	−1	1	95.07	95.16
7	50	30	20	−1	1	1	69.91	70.07
8	100	30	20	1	1	1	88.87	88.88
9	32.96	20	15	−2	0	0	51.29	51.84
10	117.04	20	15	2	0	0	80.21	79.85
11	75	3.18	15	0	−2	0	96.04	96.67
12	75	36.82	15	0	2	0	83.76	83.31
13	75	20	6.59	0	0	−2	85.14	85.05
14	75	20	23.41	0	0	2	92.45	92.73
15	75	20	15	0	0	0	93.65	93.13
16	75	20	15	0	0	0	93.28	93.13
17	75	20	15	0	0	0	93.91	93.13
18	75	20	15	0	0	0	92.45	93.13
19	75	20	15	0	0	0	92.32	93.13
20	75	20	15	0	0	0	93.19	93.13

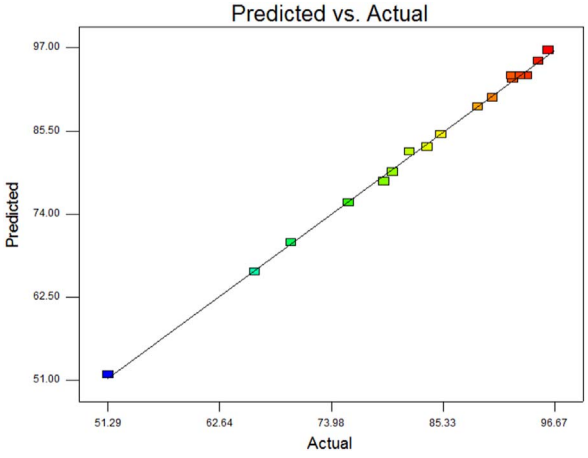

Fig. 7. Experimental values ploted againgst the predicted values derived from the model.

the model terms are not significant. The “lack of fit value” of 1.22 implied that the lack of fit is not significant relative to pure error. The non-significant lack of fit confirmed the good predictability of the model. The “predicted *R*-squared” of 0.9913 was in reasonable agreement with the “adjusted R-squared” of 0.9967, confirming good predictability of the model. It observed that among the three parameter studied, the catalyst dose (X_1) had the largest effect on the degradation of safranin-O dye to the maximum *F* value followed in order by initial dye concentration and reaction time.

3.4. Analysis of contour and response surface plots

By using the Design Expert 7.1 software, three-dimensional (3D) surface can be introduced as graphical representation of the regression equation to determine the optimum values of variables and also, their corresponding two-dimensional (2D) contour plots were fabricated. These 3D and 2D plots are widely used to achieve better understandings of the interactions between variables within the range [51,52]. The interactions between the three independent variables and the response are shown in Fig. 10. The circular nature of the contour plots shows that the interaction is negligible whereas the elliptical contour plots shows significant interaction between the corresponding variables [53]. In each plot, the effects of two parameters were varied within the experimental ranges and the other parameters fixed to zero level.

Fig. 8(a) shows the effect of catalyst dose and initial dye concentration on the degradation of safranin-O dye from aqueous solution. Catalyst dose is an important factor that significantly influence the photocatalytic degradation of dye molecules. From the figure, it is concluded that the degradation of dye increases as catalyst dose increases. This increase is

Please cite this article as: B. Ekka, et al., Titania coated silica nanocomposite prepared via encapsulation method for the degradation of Safranin-O dye from aqueous solution: Optimization using statistical design, Water Resources and Industry (2016), http://dx.doi.org/10.1016/j.wri.2016.08.001

Table 3
ANOVA results for the response surface.

Source	Sum of squares	Degree of freedom	Mean square	F value	p-value Prob > F
Model	2584.20	9	287.13	638.22	< 0.0001
A-Catalyst Dose	946.73	1	946.73	2104.32	< 0.0001
B-Dye Concentration	215.44	1	215.44	478.86	< 0.0001
C-Reaction Time	71.11	1	71.11	158.07	< 0.0001
AB	2.34	1	2.34	5.21	0.0456
AC	2.32	1	2.32	5.16	0.0464
BC	0.68	1	0.68	1.51	0.2475
A^2	1341.15	1	1341.15	2980.99	< 0.0001
B^2	17.71	1	17.71	39.37	< 0.0001
C^2	32.39	1	32.39	72.00	< 0.0001
Residual	4.50	10	0.45		
Lack of Fit	2.48	5	0.50	1.22	0.4151
Pure Error	2.02	5	0.40		
Core Total	2588.70	19			

$R^2 = 0.9983$; Adj. $R^2 = 0.9967$; Predicted $R^2 = 0.9913$

attributed to several factors such as active sites on the surface of nanoparticle, the penetration of UV light into the aqueous solution of mixture of the catalyst and dye [54]. For instance, the greater amount of photocatalyst creates more number of active radicals by absorbing the larger amount of photons that result in high efficiency of degradation [55]. In contrast to catalyst dose, photocatalytic degradation decreases with increase in dye concentration. The opposite effect is attributed to first, more number of dye molecules are adsorbed on the surface of catalyst as the concentration of the dye increases, second the generation of hydroxyl radicals is reduced as the active sites are occupied by the dye molecules and finally, the mean free path of the light in the solution decreases [56].

Fig. 8(b) represents the effect of both dye concentration and reaction time on safranin-O degradation. It is important from both mechanistic and application point of view to predicting the dependence of the photocatalytic reaction rate on the dye concentration. It is generally known that the rate of degradation increases with increase in dye concentration to a certain level and further increase in dye concentration leads to opposite effect [57] and it could be due to the lack of available active sites required for the high dye concentration. It concludes that as the concentration of the dye increases, more number of dye molecules get adsorbed on the surface of the catalyst as a result, the requirement of the reactive species such as $O\dot{H}$ and O_2- needed for the degradation of the dye also increases. For a constant catalyst dose and reaction time, the formation of $O\dot{H}$ and O_2- on the surface of catalyst remains constant. Hence, the available hydroxyl radicals are inadequate for the degradation of the dye at higher concentrations. Therefore, the degradation efficiency decreases with increase in dye concentration. Furthermore, the absorption of photon by safranin-O dye itself reduces the production of hydroxyl radicals on the surface of catalyst. Moreover, degradation intensity also related to irradiation intensity. As the radiation increases, degradation of dye also increase [58]. Thus, at higher dye concentration, degradation decreases at sufficiently long distances from the light source due to the retarding of the penetration of light. Hence, it is confirmed that as the initial dye concentration increases, the requirement of catalyst surface needed for the degradation also increases [59]. In addition, degradation of safranin-O increases with increase in reaction time.

Fig. 8(c) finally, shows the effect of catalyst dose and reaction time on the degradation of safranin-O dye. Degradation efficiency increases with increase in reaction time whereas it decreases with increase in catalyst dose. This may be due to the turbidity of the suspension, at a higher amount of catalyst.

3.5. Determination of optimal condition for photocatalytic degradation of dyes

The main objective of the optimization in this work is to effectively obtain the optimum values of variables for photocatalytic degradation efficiency of the dye based on the experimental results, by using numerical optimization methods in the Design Expert 7.1 software. The desired goals for all the variables are chosen in the experimental ranges and these are the amount of titania coated silica nanoparticles (50–100 mg), initial dye concentration (10–40 mg/L) and the reaction time (10–20 min). The optimum values of the variables for the maximum decolourization efficiency were found to be 89.80 mg (X_1), 17.61 mg/L (X_2) and 12 min (X_3) respectively (shown in Table 4). Using these values, we have degraded the safranin-O dye analytically and the degradation was 93.29%. These results confirm that the RSM for the decolourization efficiency is validated and can be successfully used in future studies.

Please cite this article as: B. Ekka, et al., Titania coated silica nanocomposite prepared via encapsulation method for the degradation of Safranin-O dye from aqueous solution: Optimization using statistical design, Water Resources and Industry (2016), http://dx.doi.org/10.1016/j.wri.2016.08.001

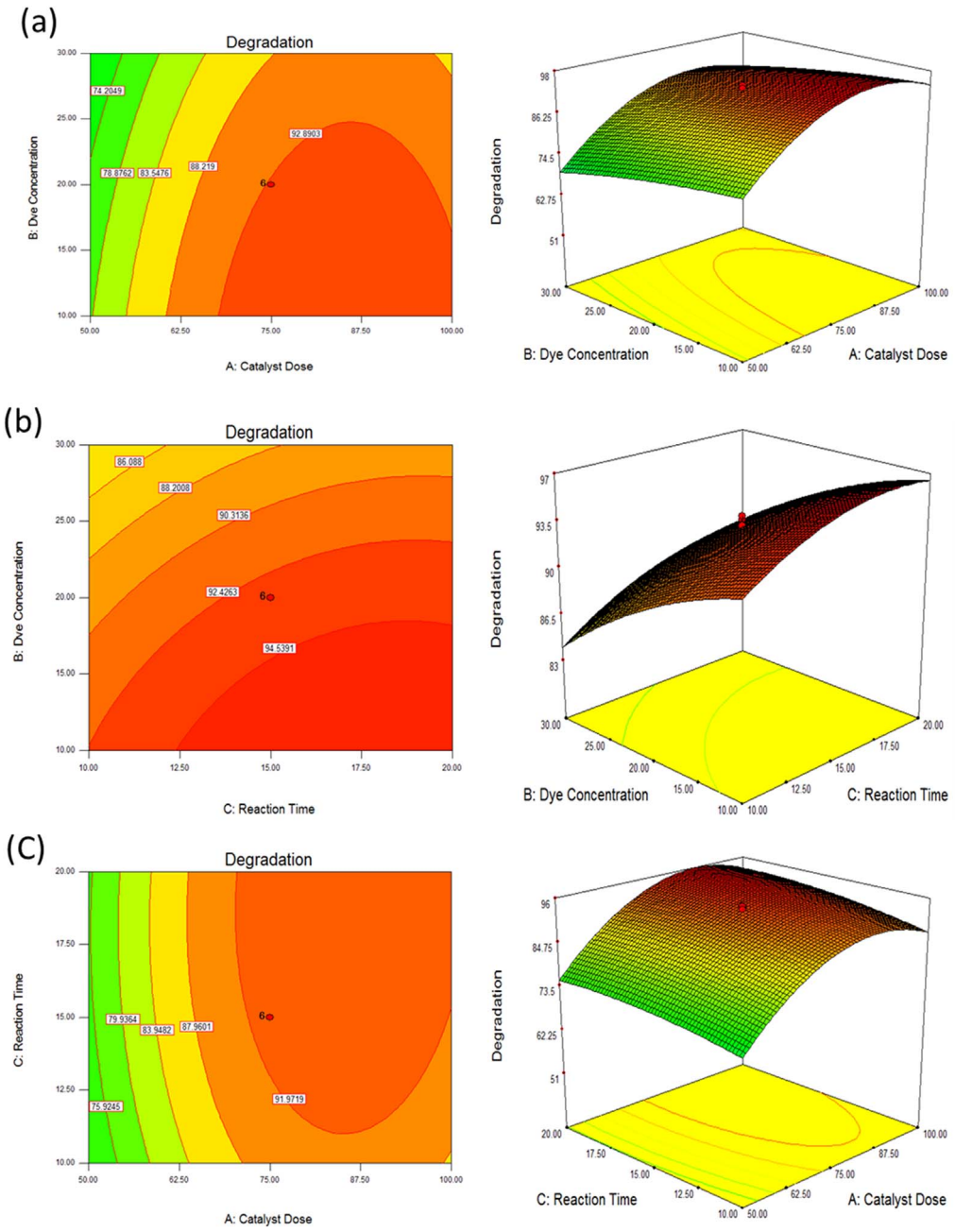

Fig. 8. The contour and response surface plots of degradation efficiency titania coated silica nanoparticle photocatalyst as the function of (a) catalyst dose with dye concentartion, (b) reaction time with dye concentartion, (c) catalyst dose with reaction time.

Table 4
The critical values of variables for the optimal decolorization efficiency.

Parameters	Critical values
Catalyst Dose (mg/g)	89.80
Initial Dye Concentration (mg/L)	17.61
Reaction Time (min)	12
Degradation (%)	93.29

Please cite this article as: B. Ekka, et al., Titania coated silica nanocomposite prepared via encapsulation method for the degradation of Safranin-O dye from aqueous solution: Optimization using statistical design, Water Resources and Industry (2016), http://dx.doi.org/10.1016/j.wri.2016.08.001

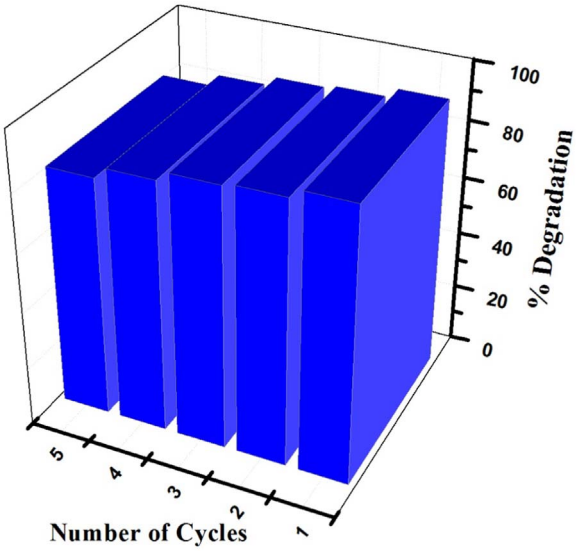

Fig. 9. Five cycles of the degradation of safranin-O using titania coated silica nanoparticle as the photocatalyst under UV-light irradiation for 20 min.

3.6. Reusability study

In order to make the degradation process more economical and feasible, potentiality of regeneration of and reusability of titania coated silica nanoparticle were studied. It is crucial to evaluate the stability of the photocatalyst for various applications. To verify the reusability of the catalyst, repeated experiments were carried out for degradation of safranin-O. After the completion of every cycle, the solution containing dye and catalyst were centrifuged and washed off with deionized water for 3–4 times to regenerate the catalyst. The catalyst was dried in an oven at 150 °C for 3 h and it was kept for reuse in next cycle. Fig. 9 shows the five cycles of degradation of dye using photocatalyst under UV light irradiation for 20 min. The results indicated that the capacity of the dye decreased with increase in the number of cycles and at the end of the fifth cycle, 82% of the degradation was obtained for the dye molecules. Therefore, titania coated silica nanoparticles is a good reusable catalyst and could be successfully used for the degradation of dye molecules from water and wastewater.

3.7. Reaction mechanism of the photocatalyst

Pure TiO_2 nanoparticles exhibited a poor photocatalytic activity under UV light in comparison with titania coated silica nanoparticles for safranin-O degradation. The activity of photocatalytic decolourization reaction depends on various factors, such as the adsorption of dye molecules at the surface of the catalyst, specific surface area of the catalyst, particles size, crystallinity and electron-hole recombination rate [60]. Irradiation of UV light on TiO_2 particles results in the promotion of an electron from the valence band to the conduction band of the particle. The consequence of this process is a region of positive charge, called as a hole (h^+), in the valance band and a free electron (e^-) in the conduction band. This h^+ can react with surface bound-hydroxyl group (OH^-) to form hydroxyl radicals ($\dot{O}H$). Furthermore, the excited electron (e^-) then

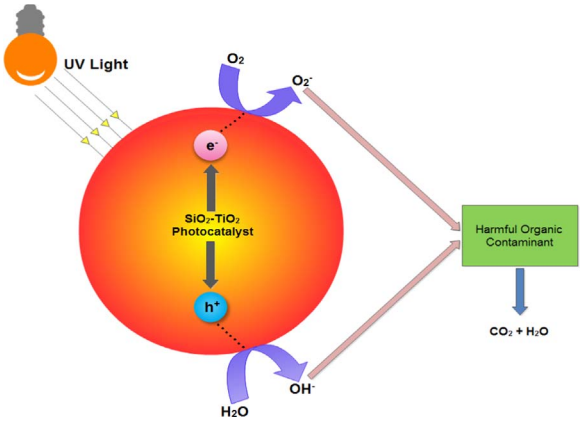

Fig. 10. Schematic diagram for UV light photocatalytic mechanism of titania coated silica nanoparticles.

Please cite this article as: B. Ekka, et al., Titania coated silica nanocomposite prepared via encapsulation method for the degradation of Safranin-O dye from aqueous solution: Optimization using statistical design, Water Resources and Industry (2016), http://dx.doi.org/10.1016/j.wri.2016.08.001

Table 5
Comparison of percentage degradation for safranin-O with other catalyst.

Catalyst	Degradation (%)	Reference
ZnS nanoparticles	51%	[60]
TiO_2 nanoparticles	60%	[61]
Ag-TiO_2 nanoparticles	96%	[61]
TiO_2 coated SiO_2 nanoparticles	93%	Present study

reacts with oxygen molecules to form superoxide ($\dot{O}_2$). The final product of the reduction is commonly hydroxyl radicals ($^{\bullet}$OH) and superoxide ($\dot{O}_2$).

Hydroxyl radicals and superoxides are known to be powerful oxidizing agents and on this property, they can react with organic pollutants, adsorbed onto the catalyst surface during the photocatalytic process.

Typical mechanism of the degradation process includes:

$$TiO_2 + h\nu \rightarrow h^+ + e^-$$
$$e^- + O_2 \rightarrow {}^{\bullet}O_2^-$$
$${}^{\bullet}O_2^- + 2H^+ + e^- \rightarrow OH + OH^-$$
$$H_2O + h^+ \rightarrow OH + H^+$$
$$OH^- + h^+ \rightarrow {}^{\bullet}OH$$
$${}^{\bullet}O_2^- + SO \rightarrow \textit{degradation products}$$
$${}^{\bullet}OH + SO \rightarrow \textit{degradation products}$$

In this work, we found that the degradation of safranin-O of pure TiO_2 was lower as compared to titania coated silica nanoparticles. This may be due to the higher surface area of silica nanoparticle. The degradation mechanism of the safranin-O dye has been shown in Fig. 10.

3.8. Comparative study

The comparative study for decolourization of safranin-O using titania coated silica nanoparticles and other photocatalyst are given in Table 5. From Table 5, it was confirmed that the degradation efficiency of safranin-O using titania coated silica nanoparticles are greater than ZnS, TiO_2, Bi_2O_3, AgBr/BiOBr hybrid material and $NaTaO_3$:La powder [61–66] and further implied that the catalyst studied in this work has the potential to degrade the organic pollutants from aqueous solutions.

4. Conclusions

Titania coated silica nanoparticles were successfully prepared by a nanoparticle encapsulation method. Synthesized catalyst was characterized with several characterization techniques such FT-IR, XRD, FESEM, N_2 adsorption-desorption and zeta potential measurements. For the first time, the response surface methodology was applied to optimize the parameters in the photocatalytic degradation of safranin-O using titania coated silica nanoparticle. A quadratic model represents the functional relationship between the degradation of dye and three independent variables: catalyst dose, dye concentration and reaction time. Among all the parameters in the experimental design, the catalyst dose played the most important role to influence the degradation activity. Meanwhile, other two parameters such as dye concentration and reaction time also showed the influence to the photocatalytic degradation efficiency of the photocatalyst. Under the optimized conditions of 89.80 mg/g catalyst dose, 17.61 mg/L initial dye concentration and 12 min, the degradation efficiency of safranin-O approached 93.29%. Regression coefficient (R^2=0.9983) of experimental results showed a good agreement with the predicted values.

Acknowledgments

The authors are thankful to Ministry of Human Resource Development (MHRD), Govt. of India for funding; and the required analytical instrument facility.

References

[1] A.M. Talarposhti, T. Donnelly, G.K. Anderson, Colour removal from a simulated dye wastewater using a two-phase anaerobic packed bed reactor, Water Resour. 35 (2001) 425–432.
[2] A.Bd Santos, F.J. Cervantes, J.Bv Lier, Review paper on current technologies for decolourisation of textile wastewaters: perspectives for anaerobic biotechnology, Bioresour. Technol. 98 (2007) 2369–2385.

Please cite this article as: B. Ekka, et al., Titania coated silica nanocomposite prepared via encapsulation method for the degradation of Safranin-O dye from aqueous solution: Optimization using statistical design, Water Resources and Industry (2016), http://dx.doi.org/10.1016/j.wri.2016.08.001

[3] S. Srivastava, R. Sinha, D. Roy, Toxicological effects of malachite green, Aqua. Toxicol. 66 (2004) 319–329.
[4] J. Li, Y. Xu, Y. Liu, D. Wu, Y. Sun, Synthesis of hydrophilic ZnSn a nanocrystals and their application in photocatalytic degradation of dye pollutants, China Part. 2 (2004) 266–269.
[5] W. Cheng, S.G. Wang, L. Lu, W.X. Gong, X.W. Liu, B.Y. Gao, H.Y. Zhang, Removal of malachite green (MG) from aqueous solutions by native and heat-treated anaerobic granular sludge, Biochem. Eng. J. 39 (2008) 538–546.
[6] G. Crini, Non-conventional low-cost adsorbents for dye removal: a review, Bioresour. Technol. 97 (2006) 1061–1085.
[7] H.J. Hsing, P.C. Chiang, E.E. Chang, M.Y. Chen, The decolorization and mineralization of Acid Orange 6 azo dye in aqueous solution by advanced oxidation processes: a comparative study, J. Hazard. Mater. 141 (2007) 8–16.
[8] D. Roy, K.T. Valsaraj, S.A. Kottai, Separation of organic dyes from wastewater by using colloidal gas aphrons, Sep. Sci. Technol. 27 (1992) 573–588.
[9] D. Pak, W. Chang, Color and suspended solid removal with a novel coagulation technology, Water Sci. Technol.: Water Supply 2 (2002) 77–81.
[10] A. Aleboyeh, H. Aleboyeh, Y. Moussa, Critical effect of hydrogen peroxide in photochemical oxidative decolorization of dyes: Acid Orange 8, Acid Blue 74 and Methyl Orange, Dyes Pigment. 57 (2003) 67–75.
[11] G. Parshetti, S. Kalme, G. Saratale, S. Govindwar, Biodegradation of malachite green by Kocuria rosea MTCC 1532, Acta Chim. Slov. 53 (2006) 492–498.
[12] Y. Ju, S. Yang, Y. Ding, C. Sun, A. Zhang, L. Wang, Microwave-assisted rapid photocatalytic degradation of malachite green in TiO_2 suspensions: mechanism and pathways, J. Phys. Chem. A 112 (2008) 11172–11177.
[13] J.K. Lee, J.H. Gu, M.R. Kim, H.S. Chun, Incineration characteristics of dye sludge in a fluidized bed incinerator, J. Chem. Eng. Jpn. 34 (2001) 171–175.
[14] J.G. Montano, X. Domenech, J.A. Garcia-Hortal, F. Torrades, P. Peral, The testing of several biological and chemical coupled treatments for Cibacron Red FN-R azo dye removal, J. Hazard. Mater. 154 (2008) 484–490.
[15] A.G.S. Prado, E.A. Faria, J.R. SouzaDe, J.D. Torres, Ammonium complex of niobium as a precursor for the hydrothermal preparation of cellulose acetate/Nb_2O_5 photocatalyst, J. Mol. Catal. A 237 (2005) 115–119.
[16] J.D. Torres, E.A. Faria, J.R. SouzaDe, A.G.S. Prado, Preparation of photoactive chitosan–niobium (V) oxide composites for dye degradation, J. Photochem. Photobiol. A 182 (2006) 202–206.
[17] A.G.S. Prado, E.A. Faria, J.R. SouzaDe, J.D. Torres, Ammonium complex of niobium as a precursor for the hydrothermal preparation of cellulose acetate/Nb_2O_5 photocatalyst, J. Mol. Catal. A 237 (2005) 115–119.
[18] J.D. Torres, E.A. Faria, J.R. SouzaDe, A.G.S. Prado, Preparation of photoactive chitosan–niobium (V) oxide composites for dye degradation, J. Photochem. Photobiol. A 182 (2006) 202–206.
[19] M.R. Hoffman, S.T. Martin, W. Choi, W. Bahnemann, Environmental applications of semiconductor photocatalysis, Chem. Rev. 95 (1995) 69–96.
[20] A.G.S. Prado, L.B. Bolzon, C.P. Pedroso, A.O. Moura, L.L. Costa, Nb_2O_5 as efficient and recyclable photocatalyst for indigo carmine degradation, Appl. Catal. B 82 (2008) 219–224.
[21] S. Sakthivel, B. Neppolian, B. Arabindoo, M. Palanichamy, V. Murugesan, Photocatalytic degradation of leather dye over ZnO catalyst supported on alumina and glass surfaces, Water Sci. Technol. 44 (2001) 211–218.
[22] M.T. Uddin, Y. Nicolas, C. Olivier, T. Toupance, L. Servant, M.M. Müller, H.J. Kleebe, J. Ziegler, W. Jaegermann, Nanostructured SnO_2-ZnO heterojunction photocatalysts showing enhanced photocatalytic activity for the degradation of organic Dyes, Inorg. Chem. 51 (2012) 7764–7773.
[23] A.G.S. Prado, L.B. Bolzon, C.P. Pedroso, A.O. Moura, L.L. Costa, Nb_2O_5 as efficient and recyclable photocatalyst for indigo carmine degradation, Appl. Catal. B: Environ. 82 (2008) 219–224.
[24] W. Zhao, W. Ma, C. Chen, J. Zhao, Z. Shuai, Efficient degradation of toxic organic pollutants with Ni2O3/TiO2−xBx under visible irradiation, J. Am. Chem. Soc. 126 (2004) 4782–4783.
[25] J. Yang, X. Wang, J. Dai, J. Li, Efficient visible-light-driven photocatalytic degradation with Bi_2O_3 coupling silica doped TiO_2, Ind. Eng. Chem. Res. 53 (2014) 12575–12586.
[26] W. Kim, T. Tachikawa, T. Majima, W. Choi, Photocatalysis of dye-sensitized TiO_2 nanoparticles with thin overcoat of Al_2O_3: enhanced activity for H_2 production and dechlorination of CCl_4, J. Phys. Chem. C 113 (2009) 10603–10609.
[27] T. Aarthi, G. Madras, Photocatalytic degradation of rhodamine dyes with Nano-TiO_2, Ind. Eng. Chem. Res. 46 (2007) 7–14.
[28] K. Nagaveni, M.S. Hegde, N. Ravishankar, G.N. Subbanna, G. Madras, Synthesis and structure of nanocrystalline TiO_2 with lower band gap showing high photocatalytic activity, Langmuir 20 (2004) 2900–2907.
[29] S. Liu, J. Yu, M. Jaroniec, Tunable photocatalytic selectivity of hollow TiO_2 microspheres composed of anatase polyhedra with exposed {001} facets, J. Am. Chem. Soc. 132 (2010) 11914–11916.
[30] S. Kamaruddin, D. Stephan, The preparation of silica–titania core–shell particles and their impact as an alternative material to pure nano-titania photocatalysts, Catal. Today 161 (2011) 53–58.
[31] A.K. Gupta, A. Pal, C. Sahoo, Photocatalytic degradation of a mixture of Crystal Violet (Basic Violet 3) and Methyl Red dye in aqueous suspensions using AgC doped TiO_2, Dyes Pigment. 69 (2006) 224–232.
[32] C. Hu, Y. Lan, J. Qu, X. Hu, A. Wang, Ag/AgBr/TiO_2 visible light photocatalyst for destruction of azo dyes and bacteria, J. Phys. Chem. B 110 (2006) 4066–4072.
[33] A.T. Kuvarega, R.W.M. Krause, B.B. Mamba, Nitrogen/palladium-codoped TiO_2 for efficient visible light photocatalytic dye degradation, J. Phys. Chem. C. 115 (2011) 22110–22120.
[34] Y. Cong, J. Zhang, F. Chen, M. Anpo, Synthesis and characterization of nitrogen-doped TiO_2 nanophotocatalyst with high visible light activity, J. Phys. Chem. C. 111 (2007) 6976–6982.
[35] D. Chen, Z. Jiang, J. Geng, Q. Wang, D. Yang, Carbon and nitrogen co-doped TiO_2 with enhanced visible-light photocatalytic activity, Ind. Eng. Chem. Res. 46 (2007) 2741–2746.
[36] J.W. Lee, M.R. Othman, Y. Eom, T.G. Lee, W.S. Kim, J. Kim, The effects of sonification and TiO_2 deposition on the micro-characteristics of the thermally treated SiO_2/TiO_2 spherical core–shell particles for photo-catalysis of methyl orange, Microporous Mesoporous Mater. 116 (2008) 561–568.
[37] H. Takahashi, B. Li, T. Sasaki, C. Miyazaki, T. Kajino, S. Inagaki, Catalytic activity in organic solvents and stability of immobilized enzymes depend on the pore size and surface characteristics of *meso*porous Silica, Chem. Mater. 12 (2000) 3301–3305.
[38] Y. Zhao, B.G. Trewyn, I.I. Slowing, V.S.Y. Lin, *meso*porous Silica nanoparticle-based double drug delivery system for glucose-responsive controlled release of insulin and cyclic AMP, J. Am. Chem. Soc. 131 (2009) 8398–8400.
[39] S. Mandal, D. Roy, R.V. Chaudhari, M. Sastry, Pt and Pd nanoparticles immobilized on amine-functionalized zeolite: excellent catalysts for hydrogenation and heck reactions, Chem. Mater. 16 (2004) 3714–3724.
[40] J.S. Kwak, Application of Taguchi and response surface methodologies for geometric error in surface grinding process, Int. J. Mach. Tool. Manuf. 45 (2005) 327–334.
[41] N. Aslan, Application of response surface methodology and central composite rotatable design for modeling and optimization of a multi-gravity separator for chromite concentration, Powder Technol. 185 (2008) 80–86.
[42] G.E.P. Box, W.G. Hunter, The 2k-p fractional factorial designs, J. Technometr. 3 (1961) 311–458.
[43] A.R. Khataee, M. Fathinia, S. Aber, M. Zarei, Optimization of photocatalytic treatment of dye solution on supported TiO_2 nanoparticles by central composite design: intermediates identification, J. Hazard. Mater. 181 (2010) 886–897.
[44] Z.Y. Liu, X. Quan, H.P. Fu, X.Y. Li, K. Yang, Effect of embedded-silica on microstructure and photocatalytic activity of titania prepared by ultrasound-assisted hydrolysis, Appl. Catal. B 52 (2004) 33–40.
[45] O.K. Park, Y.S. Kang, Preparation and characterization of silica-coated TiO_2 nanoparticle, Colloid. Surf. A: Physicochem. Eng. Asp. 257 (2005) 261–265.
[46] Y. Li, S. Kim, Synthesis and characterization of nano titania particles embedded in mesoporous silica with both high photocatalytic activity and adsorption capability, J. Phys. Chem. B 109 (2005) 12309–12315.
[47] K. Shankar, G.K. Mor, H.E. Prakasam, O.K. Varghese, C.A. Grimes, Self-assembled hybrid Polymer-TiO_2 nanotube array heterojunction solar cells,

Please cite this article as: B. Ekka, et al., Titania coated silica nanocomposite prepared via encapsulation method for the degradation of Safranin-O dye from aqueous solution: Optimization using statistical design, Water Resources and Industry (2016), http://dx.doi.org/10.1016/j.wri.2016.08.001

Langmuir 23 (2007) 12445–12449.
[48] T.P. Ang, C.S. Toh, Y.F. Han, Synthesis, characterization, and activity of visible-light-driven nitrogen-doped TiO_2-SiO_2 mixed oxide photocatalysts, J. Phys. Chem. C. 113 (2009) 10560–10567.
[49] J. Bahadur, D. Sen, S. Mazumder, P.U. Sastry, B. Paul, H. Bhatt, S.G. Singh, One-step fabrication of thermally stable tio2/sio2 nanocomposite microspheres by evaporation-induced self-assembly, Langmuir 28 (2012) 11343–11353.
[50] S. Kamaruddin, D. Stephan, The preparation of silica-titania core-shell particles and their impact as an alternative material to pure nano-titania photocatalysts, Catal. Today 161 (2011) 53–58.
[51] H.L. Liu, Y.R. Chiou, Optimal decolorization efficiency of Reactive Red 239 by UV/TiO_2 photocatalytic process coupled with response surface methodology, Chem. Eng. J. 112 (2005) 173–179.
[52] D. Vildozo, C. Ferronato, M. Sleiman, J.M. Chovelon, Photocatalytic treatment of indoor air: optimization of 2-propanol removal using a response surface methodology (RSM), Appl. Catal. B 94 (2010) 303–310.
[53] J. Fan, C. Yi, X. Lan, B. Yang, Optimization of synthetic strategy of 4′4″(5″)-Di-*tert*-butyldibenzo-18-crown-6 using response surface methodology, Org. Process Res. Dev. 17 (2013) 368–374.
[54] M.S.T. Goncalves, A.M.F. Oliveira-Campos, E.M.M.S. Pinto, P.M.S. Plasencia, M.J.R.P. Queiroz, Effect of embedded-silica on microstructure and photocatalytic activity of titania prepared by ultrasound-assisted hydrolysis, Chemosphere 39 (1999) 781–786.
[55] Y. Liu, Y. Ohko, R. Zhang, Y. Yang, Z. Zhang, Degradation of malachite green on Pd/WO_3 photocatalysts under simulated solar light, J. Hazard. Mater. 184 (2010) 386–391.
[56] E.M. Saggioro, A.S. Oliviera, T. Pavesi, C.G. Maia, Use of Titanium Dioxide photocatalysis on the remediation of model textile wastewaters containing azo dyes, Molecules 16 (2011) 10370–10386.
[57] M. Saquib, M. Muneer, TiO_2-mediated photocatalytic degradation of a triphenylmethane dye (gentian violet), in aqueous suspensions, Dyes Pigment. 56 (2003) 37–49.
[58] L. Zhang, C.Y. Liu, X.M. Ren, Solar light induced and TiO_2 assisted degradation of textile dye reactive blue 4, J. Photochem. Photobiol. A 85 (1995) 239–245.
[59] B. Neppolian, H.C. Choi, S. Sakthivel, B. Arabindoo, V. Murugesan, Solar light induced and TiO_2 assisted degradation of textile dye reactive blue 4, Chemosphere 46 (2002) 1173–1181.
[60] Y. Xia, L. Yin, Core–shell structured α-Fe_2O_3@TiO_2 nanocomposites with improved photocatalytic activity in the visible light region, Phys. Chem. Chem. Phys. 15 (2013) 18627–18634.
[61] M. El-Kemary, H. El-Shamy, Fluorescence modulation and photodegradation characteristics of safranin O dye in the presence of ZnS nanoparticles, J. Photochem. Photobiol. A: Chem 205 (2009) 151–155.
[62] M. El-Kemary, Y. Abdel-Moneam, M. Madkour, I. El-Mehasseb, Enhanced photocatalytic degradation of Safranin-O by heterogeneous nanoparticles for environmental applications, J. Lumin. 131 (2011) 570–576.
[63] V. Janaki, B.-T. Oh, K. Shanthi, K.-J. Lee, A.K. Ramasamy, S.K. Kannan, Efficiency of various semiconductor catalysts for photodegradation of Safranin-T, Res. Chem. Intermed. 38 (2012) 1431–1442.
[64] C. Cheng, Y. Ni, X. Ma, J. Hong, AgBr nanoparticles-improved photocatalytic property of BiOBr nanosheets, Mater. Lett. 79 (2012) 273–276.
[65] X. Li, J. Zang, Hydrothermal synthesis and characterization of Lanthanum-doped $NaTaO_3$ with high photocatalytic activity, Catal. Commun. 12 (2011) 1380–1383.
[66] K. Hayat, M.A. Gondal, M.M. Khaled, Z.H. Yamanib, S. Ahmed, Laser induced photocatalytic degradation of hazardous dye (Safranin-O) using self synthesized nanocrystalline WO_3, J. Hazard. Mater. 186 (2011) 1226–1233.

Please cite this article as: B. Ekka, et al., Titania coated silica nanocomposite prepared via encapsulation method for the degradation of Safranin-O dye from aqueous solution: Optimization using statistical design, Water Resources and Industry (2016), http://dx.doi.org/10.1016/j.wri.2016.08.001